Toxicity-specific peripheral blood T and B cell dynamics in anti-PD-1 and combined immune checkpoint inhibition

Mick J.M. van Eijs,[1,2,#] Rik J. Verheijden,[1] Stefanie A. van der Wees,[2] Stefan Nierkens,[2,3] Anne S.R. van Lindert,[4] Karijn P.M. Suijkerbuijk[1,*], Femke van Wijk;[2,*] on behalf of the UNICIT Consortium[†]

[1] Department of medical oncology, University Medical Center Utrecht, Utrecht, the Netherlands
[2] Center for Translational Immunology, University Medical Center Utrecht, Utrecht, the Netherlands
[3] Princess Máxima Center for Pediatric Oncology, Utrecht, the Netherlands
[4] Department of pulmonology, University Medical Center Utrecht, Utrecht, the Netherlands

* Contributed equally
[#] Corresponding author: Mick J.M. van Eijs. Internal mail no. KC.02.085.2, P.O. Box 85090, 3508 AB, Utrecht, the Netherlands; T: +31 (0)88 757 7183; E: m.j.m.vaneijs-2@umcutrecht.nl

[†] **Collaborators UNICIT consortium**: Linde Meyaard, Jürgen H.E. Kuball, Bas Oldenburg, Jeanette H.W. Leusen.

Abstract

Immune checkpoint inhibitors (ICI) have revolutionized the treatment landscape of advanced malignancies, but come with a diverse spectrum of immune-related adverse events (irAEs). Mechanistic studies can aid the transition from expert-opinion to evidence-based irAE treatment strategies. We aimed to longitudinally characterize peripheral blood T and B cell dynamics in ICI-treated patients by multicolor flow cytometry and serum multiplex immunoassay at baseline, ±3 weeks and ±6 weeks or upon clinically relevant irAEs. We analyzed samples from 44 ICI-treated patients (24 anti-PD-1 monotherapy, 20 combined anti-PD-1/anti-CTLA-4; cICI), of whom 21 developed irAEs, and 10 healthy donors. IrAEs after cICI were characterized by significantly enhanced proliferation of Th1-associated, mainly ($CD4^+$) effector memory T cells, as well as Th17-associated immune responses and germinal center activation (reflected by CXCL13 and IL-21 increases). We observed no changes in $CD21^{lo}$, memory, class-switched or newly activated B cell subsets. Especially double-positive $PD\text{-}1^+LAG\text{-}3^+$ $CD8^+$ T cells showed enhanced cytotoxic capacity in patients with irAEs after cICI. Within anti-PD-1 monotherapy, irAEs were associated with modestly enhanced Th1-associated responses reflected by increased serum CXCL9 and CXCL10. In conclusion, ICI-induced toxicity is dominated by enhanced Th1-associated responses, but in cICI we also found evidence for Th17-associated responses and germinal center activation. Together, our data add to the growing body of evidence that irAEs may be driven by newly activated $CD4^+$ helper T cells, specifically after cICI. This study also supports tailored irAE treatment, based on ICI regimen, and to deploy specific strategies such as Th17 inhibition especially in cICI-associated irAEs.

Keywords: Immune checkpoint inhibitors, Immune-related adverse event, peripheral blood, immunophenotyping, T and B lymphocytes.

Introduction

Immune checkpoint inhibitors (ICI) have realized unprecedented survival improvements in a selection of patients with advanced malignancies, but comes with a broad spectrum of immune-related adverse events (irAEs) [1]. To date, recommendations for irAE management are largely based on multidisciplinary expert consensus [2-4]. In quest of rationally developed treatment strategies, it has been suggested to draw on experience with specific autoimmune diseases (AD) these irAEs mimic, assuming shared pathophysiology [1]. Despite similarities, immune-related toxicity should clinically be considered a separate disease entity, for instance illustrated by the more acute onset and possibility of complete irAE reversibility with adequate therapy. Together with the concern that targeted immunosuppression may thwart antitumor immunity [5, 6], these observations underscore that evidence-based irAE treatment requires more profound biological understanding of specific mechanisms underlying ICI-induced toxicity.

Many efforts have been undertaken to predict irAEs at baseline or early on-treatment based on peripheral blood immune cells, cytokines, auto-antibodies and gut microbiome, as extensively reviewed in Hommes et al. [7]. Relatively higher blood lymphocyte count at baseline has been associated with development of irAEs [7]. Several studies that further characterized T and B cells at baseline and on-treatment reported a multitude of factors associated with irAE development, such as proliferation of (activated) $CD4^+$ and $CD8^+$ T cell subsets, baseline Th17 dominance and early increase in $CD21^{lo}$ B cells [8-12]. Most of these findings still warrant replication. Particularly effector memory $CD4^+$ T cells ($CD4_{EM}$) have recently been suggested as drivers of irAEs [10, 13, 14]. $CD4^+$ T cell clonal expansion preceding irAEs [10, 15] and indications for epitope sharing between tumor and irAE-affected tissue [16, 17] suggests a role for T cell auto-reactivity in irAE development [10, 13]. However, the concept of genuine autoimmunity does not seem to completely recapitulate the pathophysiology of irAEs.

Longitudinal studies into general irAE mechanisms comparing different ICI regimens are lacking, but urgently needed to improve irAE treatment strategies [18]. Besides, the role of B cells in irAEs has received little attention. Therefore, we interrogated peripheral T and B cell dynamics and cytokine production from baseline to several weeks on-treatment and upon immune-related toxicity in anti-PD-1 monotherapy and combined anti-CTLA-4 and anti-PD-1 (cICI) treated patients.

Methods

Study population and design

We included patients from the UNICIT biobank study conducted within the University Medical Center Utrecht (UMCU), Utrecht, the Netherlands. Adult patients undergoing a first regimen of ICI with anti-PD-1 monotherapy, combined anti-CTLA-4 and anti-PD-1 (cICI), or anti-PD-(L)1 in combination with chemotherapy for a solid malignancy are prospectively enrolled in this biobank. Stool and blood samples are collected at baseline, 3-4 weeks and 6-8 weeks after treatment initiation, and upon onset of irAEs prior to initiation of immunosuppressive therapy. Furthermore, stool and blood samples are collected after every new line immunosuppression administered for irAEs. If patients undergo diagnostic procedures for suspected immune-mediated toxicity, extra biopsies of irAE affected tissue are obtained. Tumor response to ICI per RECIST 1.1 [19], irAE incidence and severity per CTCAE version 5 [20], as well as doses and duration of all immunosuppressives administered for irAEs are continuously recorded.

Samples from patients treated with cICI or anti-PD-1 monotherapy (without chemotherapy) were used in the present study. We included peripheral blood mononuclear cell (PBMC) and serum samples collected at baseline, at 3-4 weeks, and at 6-8 weeks for patients without (NOTx) or at irAE onset for patients with clinically relevant toxicity (TOX). 'Clinically relevant toxicity' was defined as CTCAE v5 grade ≥2 irAEs leading to 1) temporary or permanent ICI discontinuation, and 2) demanding hospitalization and/or ≥0.5 mg/kg daily prednisone as first-line immunosuppression. Healthy donor PBMCs were obtained from the UMCU Mini Donor Service (MDS).

Blood sample processing and flow cytometry

PBMCs were isolated using Ficoll-Paque density-gradient centrifugation (GE Healthcare), frozen in RPMI-1640 medium (Gibco) supplemented with 2 mM L-glutamine (L-glu; Gibco), 100 IU/ml penicillin-streptomycin (p/s; Gibco), 20% fetal bovine serum (FBS; Invitrogen) and 10% DMSO (Sigma-Aldrich) and stored at -180°C. Serum was isolated and frozen at -80°C within 4 hours after blood collection.

Thawed PBMCs were plated at $0.5–1.0\times10^6$ cells per well. Prior to staining, cytokine-containing panels were restimulated with 20 ng/ml phorbol 12-myristate 13-actetate (PMA; Sigma-Aldrich) and 1.0 µg/ml ionomycin (Sigma-Aldrich; 4h, 37°C, 5% CO_2). Golgistop (0.26% monensin; BD Biosciences, 1:1,500) was added for the last 3.5h. Cells were first incubated (30min., 4°C) with eBioscience Fixable

126 Viability Dye eFluor506 (Invitrogen), washed and then incubated with the surface antibody mix
127 (**Supplementary Table 1**) in FACS buffer (phosphate buffered saline [PBS, Sigma-Aldrich], 2% FBS,
128 0.1% sodium azide; 25min., 4°C). On-treatment PD-1 expression was measured indirectly using
129 biotinylated anti-human IgG4 alone (for unstimulated) or combined with anti-PD-1 (for stimulated panels)
130 [21], followed by secondary staining with BV711-conjugated streptavidin (30min., 4°C). After fixation
131 and permeabilization with eBioscience fixation/permeabilization reagent (Invitrogen; 30min., 4°C) and
132 washing, cells were incubated (30min., 4°C) with the intracellular/intranuclear antibody mix
133 (**Supplementary Table 1**) and then measured the same or next day on an LSR Fortessa. FlowJo
134 software was used to analyze data; gating strategies are in **Supplementary Fig. 5a-b**.
135
136 **Multiplex immunoassay**
137 Concentrations of 23 soluble factors (**Supplementary Table 2**) were measured in serum collected at
138 the same timepoints as PBMCs by an in-house developed and validated immunoassay based on
139 Luminex technology (xMAP, Luminex) at the Multiplex Core Facility (UMCU) [22, 23]. Aspecific
140 heterophilic immunoglobulins were preabsorbed with heteroblock (Omega Biologicals) and acquisition
141 was performed with the Biorad FlexMAP3D (Biorad laboratories) in combination with xPONENT
142 software (v4.2, Luminex). Data was analyzed by 5-parametric curve fitting using Bio-Plex Manager
143 software (v6.1.1, Biorad). Serum samples from 10 healthy donors other than PBMC healthy donors were
144 obtained from the UMCU MDS (median age 35 years, range 26-61; 60% male sex). For one patient no
145 serum was available. Undetectable values below the limit-of-detection (LOD) were replaced with
146 0.5×LOD.
147
148 **Unsupervised and statistical analysis**
149 Analyses were performed with R version 4.2.0. For principal component analysis (PCA), missing data
150 were imputed with the population median per parameter and PCA was performed using *prcomp()* in
151 *stats* (v3.6.2) on all 159 read-out parameters across all panels. t-Distributed stochastic neighbor
152 embedding (t-SNE) projections for panel 2 (**Supplementary Table 1**) were created using *Rtsne* (θ=0.5;
153 v0.16) and k-means clustered self-organizing maps (SOMs) using FlowSOM (v2.4.0) [24] with a random
154 10% subset of pre-gated alive $CD3^+$ singlets drawn from samples upon timepoint 3, toxicity or healthy
155 donor. Longitudinal continuous data were analyzed by linear mixed effects models using the *nlme*

156 package (v3.1-158). Random intercept for subject models with fixed effects for ICI regimen, toxicity
157 status and their interaction with time were fit by restricted maximum likelihood. Significance for fixed
158 effects was evaluated with Satterthwaite approximations given relatively small sample size [25]. Model
159 output was visualized as predicted population estimates with 95% confidence intervals (CIs). Mean and
160 95% CI (by one-sample t-test) for healthy donor values was plotted as solid and dashed grey lines,
161 respectively. Continuous variables were analyzed with one-sample t tests for single groups, or a
162 Wilcoxon rank sum test (for unpaired) or Wilcoxon signed-rank test (for paired data) between two
163 groups. More than two groups were compared with the Kruskal-Wallis test followed by Dunn's post-hoc
164 test with Benjamini-Hochberg false discovery rate correction. *P* values <0.05 (two-sided) were
165 considered statistically significant.
166
167 **Ethics approval**
168 The UNICIT biobank study was not considered subject to the Dutch Medical Research with Human
169 Subjects Law by the medical research ethics committee of the UMCU. The biobank review committee
170 of the UMCU approved the UNICIT biobank protocol (TCbio 18-123) and granted permission for use of
171 human biospecimens for the present study (TCbio 19-704). All participants provided written informed
172 consent in line with the Declaration of Helsinki.
173
174 **Results**
175 **Patient characteristics**
176 Longitudinal PBMC and serum samples collected at baseline, at ±3 weeks (Timepoint 2) and at ±6
177 weeks or upon irAEs before immunosuppression (Timepoint 3/Toxicity) from 44 ICI-treated patients (11
178 anti-PD-1 monotherapy with clinically relevant irAEs [TOX], 13 anti-PD-1 monotherapy without clinically
179 relevant irAEs [NOTx], 10 combined ICI [cICI] TOX and 10 without TOX [cICI NOTx]) were included,
180 along with 10 healthy donors (HD) (**Fig. 1**, **Table 1**, **Supplementary Table 3**). As expected for cICI
181 TOX, these patients had more concomitant, earlier-onset and more severe irAEs than anti-PD-1 TOX
182 patients (**Table 1**). Baseline absolute eosinophil count, monocyte-to-lymphocyte and neutrophil-to-
183 lymphocyte ratios derived from complete blood counts were equal between TOX and NOTx patients, as
184 well as T cell-to-monocyte ratio assessed by flow cytometry.
185

186 **Table 1. Characteristics of patients and healthy donors**

	Anti-PD-1 NOTx (N=13)	Anti-PD-1 TOX (N=11)	cICI NOTx (N=10)	cICI TOX (N=10)	Healthy donor (N=10)	*P* value
Age (yr)						
Median (IQR)	63.0 (57-69)	73 (66.5-76.5)	71.0 (58.25-75)	49.5 (45.5-62.75)	56.0 (38.75-60.75)	**<0.01**
Sex (male), N (%)	9 (69.2)	8 (72.7)	10 (100)	8 (80.0)	3 (30.0)	**0.012**
Primary tumor, N (%)						
Melanoma	9 (69.2)	9 (81.8)	3 (30.0)	8 (80.0)	N/A	**<0.01**
Non-small cell lung cancer	0 (0.0)	1 (9.1)	0 (0.0)	0 (0.0)		
Renal cell carcinoma	1 (7.7)	0 (0.0)	6 (60.0)	2 (20.0)		
Urothelial cell carcinoma	3 (23.1)	0 (0.0)	0 (0.0)	0 (0.0)		
Other	0 (0.0)	1 (9.1)[a]	1 (10.0)[b]	0 (0.0)		
Tumor stage, N (%)						
III	4 (30.8)	4 (36.4)	0 (0.0)	0 (0.0	N/A	**0.031**
IV	9 (69.2)	7 (63.6)	10 (100.0)	100 (100.0)		
Time-to-toxicity (weeks)						
Median (IQR)	N/A	8.0 (6-12)	N/A	4.5 (3-6)	N/A	0.076
Number of toxicities						
1	N/A	9 (81.8)	N/A	5 (50.0)	N/A	0.28
2		2 (18.2)		2 (20.0)		
3		0 (0.0)		2 (20.0)		
>3		0 (0.0)		1 (10.0)		
Highest grade (CTCAE v5)						
II	N/A	8 (72.7)	N/A	0 (0.0)	N/A	**<0.01**
III		2 (18.2)		8 (80.0)		
IV		1 (9.1)		2 (20.0)		
Preexistent autoimmune disease, N (%)	0 (0.0)	0 (0.0)	1 (10.0)	0 (0.0)	0 (0.0)	0.45

[a]Squamous cell carcinoma of unknown primary, [b]Mismatch repair deficient colorectal cancer. Groups are compared by Kruskal-Wallis (continuous variables) or Fisher's exact test (categorical variables). Abbreviations: anti-PD-1 denotes 'anti-PD-1 monotherapy', cICI 'combined immune checkpoint inhibition', CTCAE 'Common Terminology Criteria for Adverse Events', IQR 'interquartile range', N/A 'not applicable', NOTx 'no clinically relevant irAEs', TOX 'with clinically relevant irAEs', yr 'years'.

187

188 **$CD4_{EM}$ T cell proliferation is strongly associated with irAEs in combined ICI**

189 We extensively characterized the dynamics of peripheral T and B cell immunity during ICI treatment and
190 towards the manifestation of toxicity using multicolor flow cytometry. We explored shared features
191 among subjects, with principal component analysis (PCA) with all 159 readout parameters from panels
192 in **Supplementary Table 1** pooled together. cICI TOX patients, especially on-treatment timepoints,
193 partially separated from all other subjects, including healthy donors, mainly through principal component
194 2 (**Fig. 2a**, **Supplementary Table 4**).

195 Based on the expression of CD27 and CD45RA, distributions of $CD4^+$ and $CD8^+$ T effector
196 memory (EM, $CD27^-CD45RA^-$), central memory (CM, $CD27^+CD45RA^-$), terminally differentiated
197 effector memory re-expressing CD45RA (EMRA, $CD27^-CD45RA^+$) and naive ($CD27^+CD45RA^+$)
198 subsets were analyzed. Although pre-treatment $CD4_{EM}$ frequency has been reported as irAE predictor
199 [10], baseline proportions of $CD4^+$ and $CD8^+$ T subsets were similar between TOX and NOTx patients
200 (**Supplementary Fig. 1a**). Compared to ICI-treated patients, healthy donors had fewer $CD4_{EM}$ T cells
201 and more naive $CD8^+$ T cells (**Supplementary Fig. 1a**). During ICI treatment, and even upon onset of
202 irAEs, relative frequencies of naive/memory subsets remained unchanged, except for an increase in

203 $CD8_{EM}$ T cells in cICI TOX (**Supplementary Fig. 1b**). However, group-specific differences in proliferation
204 (based on Ki67) over time were present. A significant increase in $CD4_{EM}$ proliferation from baseline to
205 Timepoint 2 was observed in all cICI TOX patients, but not in cICI NOTx patients (**Fig. 2b**). To enable
206 comparison of all five groups (TOX or NOTx in anti-PD-1 monotherapy or cICI and healthy donors)
207 simultaneously and over time, we graphically summarized patient-level data by plotting group-specific
208 linear mixed models. cICI TOX, but not NOTx or anti-PD-1-treated patients showed significantly
209 increased proliferation in $CD4_{EM}$, $CD4_{CM}$, $CD8_{EM}$, $CD8_{CM}$ and $CD8_{EMRA}$ T cells (**Fig. 2c,d**,
210 **Supplementary Fig. 1c-e**).
211 While the latter effects pertain to the (early) effects of ICI treatment, we were also interested in
212 baseline parameters associated with irAE development. Higher $CD4_{EM}$ proliferation before the first ICI
213 administration was associated with shorter time-to-toxicity (ρ = -0.53, P = 0.013), but this association
214 was entirely driven by the cICI group (ρ = -0.67, P = 0.034, **Fig. 2e**). In most cICI treated TOX patients,
215 the increase in Ki67 expression reached a plateau at 3 weeks after ICI initiation (**Fig. 2b**). Both cICI
216 TOX patients with longest time-to-toxicity developed hypophysitis, a presumably complement-mediated
217 irAE with distinct pathogenesis from most other toxicities [26]. This further strengthens the association
218 of baseline $CD4_{EM}$ proliferation with early-onset toxicity after cICI.
219
220 **Th1- and Th17-associated immune responses primarily delineate irAEs after combined ICI, while**
221 **anti-PD-1 TOX features only a modest Th1-associated response**
222 Expanding further on the $CD4^+$ compartment, we investigated immune response skewing by the
223 percentages of $CXCR3^+CCR4^-$, IFN-γ^+ and IL-17^+ $CD4^+$ T cells. Relative abundance of all three subsets
224 remained constant over time and neither correlated with ICI regimen, nor with toxicity development (data
225 not shown). Although we found no differences in the percentage of IFN-γ^+ $CD4^+$ T cells over time (**Fig.**
226 **3a**), cycling $CXCR3^+CCR4^-$ (Th1-associated) $CD45RO^+$ memory $CD4^+$ T cells were dominant in cICI
227 TOX relative to all other groups (**Fig. 3b**). Correspondingly, we observed increased proliferation of
228 $CXCR3^+$ $CD45RO^+$ memory $CD8^+$ T cells in cICI TOX patients (**Supplementary Fig. 2a**). These findings
229 were corroborated by serum multiplex data, which showed increased serum levels of Th1-associated
230 cytokines IL-12, TNF-α and IFN-γ in cICI TOX, and CXCL9 and CXCL10 both in anti-PD-1 and cICI TOX
231 upon Timepoint 3/Toxicity (**Fig. 3c,d**, **Supplementary Fig. 2b–e**).

232 We further characterized the kinetics of IL-17 producing $CD4^+$ T cells, which is especially
233 relevant since inhibition of Th17 differentiation by the IL-6 receptor blocker (IL-6RB) tocilizumab is
234 clinically being tested to uncouple ICI toxicity from efficacy [27]. After the first treatment cycle, cICI TOX,
235 but not anti-PD-1 TOX or NOTx patients demonstrated a vast increase in IL-17^+ T cells (**Fig. 3e**,
236 **Supplementary Fig. 2f**). Ki67 expression in IL-17^+ $CD4^+$ T cells was non-significantly higher in TOX
237 compared to NOTx across all timepoints, including baseline, regardless ICI regimen (**Supplementary**
238 **Fig. 2g**). The relative decrease of IL-17^+ T cells from timepoint 2 to irAE onset in cICI TOX is likely due
239 to relative expansion of other subsets, as serum concentrations of Th17-associated cytokines IL-6, IL-
240 23 and IL-17 remained stable or even increased from Timepoint 2 towards irAE onset (**Fig. 3c**,
241 **Supplementary Fig. 2c**) while IL-23 and IL-17 even show a greater than eightfold increase in cICI TOX
242 compared to cICI NOTx patients at Timepoint 3/Toxicity (**Supplementary Fig. 2e**).
243 Together, our data confirm that cICI TOX is largely Th1/Th17 driven, while anti-PD-1 TOX only
244 features modest Th1 enhancement relative to anti-PD-1 NOTx as assessed by serum multiplex data.
245 Furthermore, these human data suggest that IL-6RB therapy to mitigate ICI toxicity may be more
246 effective in cICI than in anti-PD-1 monotherapy, although preclinical models have demonstrated its
247 efficacy both in anti-CTLA-4 and anti-PD-1 monotherapies [27].
248
249 **PD-1^+LAG-3^+ $CD8^+$ T cells bear intact inflammatory and cytotoxic potential regardless**
250 **development of irAEs**
251 Next, we investigated the cytotoxic potential of $CD4^+$ and $CD8^+$ T cells in relation to co-inhibitory receptor
252 expression. We used CD95 expression to select for the antigen-experienced $CD8^+$ T cell pool [28], which
253 largely overlaps with $CD45RO^+$ memory cells but also includes T_{EMRA}s (**Fig. 4a**). First, we created t-SNE
254 and FlowSOM visualizations of $CD3^+$ T cells from Timepoint 3/Toxicity across all patients and healthy
255 donors, to explore the variety of subsets in an unbiased way. Proinflammatory cells with high potential
256 for IFN-γ production were represented mainly across the $CD8^+$ compartment (**Fig. 4b**). Within the $CD8^+$
257 compartment, granzyme B production was especially high in the subset expressing senescence marker
258 CD57 (**Fig. 4b**). Although this subset appeared brighter in the anti-PD-1 and cICI TOX density plots
259 (**Fig. 4b**), we found no statistical difference in $CD57^+$ $CD8^+$ T cell abundance between groups at
260 Timepoint 3/Toxicity. Labels assigned based on manual gating matched unsupervised clustering results,

261 demonstrating that our gating strategy adequately covers relevant biological variation (**Supplementary**
262 **Fig. 3a**).
263 Subsequentially, we investigated co-expression patterns of classical exhaustion markers PD-1 and
264 LAG-3. At baseline, PD-1$^+$LAG-3$^+$ double-positive (DP) CD8$^+$ T cells were least prevalent across groups,
265 while DP CD4$^+$ T cells were higher and made up the largest fraction of CD4$^+$ T cells in both TOX and
266 NOTx patients, compared to healthy donors (**Fig. 4c**). We found no differences in expression patterns
267 of PD-1 and LAG-3 occurring between TOX and NOTx post-treatment (**Supplementary Fig. 3b**).
268 Since merely expression of inhibitory receptors is not indicative of differentiation or functional status,
269 we assessed proinflammatory and cytotoxic capacity by measurement of IFN-γ and granzyme B
270 production after restimulation with PMA and ionomycin. Compared to double-negative (DN) T cells, a
271 much larger proportion of DP (and to a lesser extent PD-1$^+$LAG-3$^-$) CD8$^+$ T cells produced IFN-γ (**Fig.**
272 **4d**,**e**). This indicates preserved proinflammatory potential of DP cells and is supported by transcriptomic
273 data in circulating PD-1$^+$TIGIT$^+$ CD8$^+$ T cells, mostly co-expressing LAG-3, in melanoma and Merkel cell
274 carcinoma [29]. In contrast, we found that granzyme B production was drastically lower in DP relative to
275 DN CD8$^+$ T cells, regardless timepoint or the development of irAEs (**Supplementary Fig. 3c,d**). Still,
276 cICI TOX featured a profound increase in CD8$^+$ granzyme B production over time relative to other
277 groups, especially in the DP subset (**Fig. 4f**, **Supplementary Fig. 3e,f**).
278 In conclusion, our data suggest remaining cytokine production potential in supposedly senescent
279 CD57$^+$ CD8$^+$ T cells. Moreover, PD-1$^+$LAG-3$^+$ DP CD8$^+$ T cells retain their proinflammatory and cytotoxic
280 potential, while towards irAEs after cICI the fraction of granzyme B producing cells increases especially
281 in this DP subset.
282
283 **No changes in B cell subsets are observed, but serum cytokine levels indicate germinal center**
284 **activation in combined ICI TOX**
285 Then we set out to analyze the CD19$^+$ B cell compartment over time. Although early increase in CD21^{lo}
286 B cells (mainly representing a memory subset) has been associated with irAEs following cICI [11, 30],
287 we found no changes in CD21^{lo} B cells following ICI, while CD27$^+$ memory B cells in cICI TOX even
288 decreased (**Fig. 5a,b**). Moreover, we observed no B cell activation, measured by CCR6 expression
289 (**Supplementary Fig. 4a**). The fraction of IgM$^-$ class-switched B cells also remained unchanged over
290 time in all groups (**Supplementary Fig. 4b**). Despite lacking indications for B cell activation and

291 maturation based on flow cytometry data, increasing serum levels of APRIL, CXCL13 and IL-21 towards
292 toxicity suggest germinal center activity or tertiary lymphoid structure (TLS) formation, again especially
293 in cICI TOX (**Fig. 5c**, **Fig. 3c**, **Supplementary Fig. 2b,c**). Besides, higher $CD27^{+}CD38^{hi}$ plasmablast
294 abundance at baseline was associated with shorter time-to-toxicity in cICI TOX (**Fig. 5d**). In sum, these
295 data support a role for adaptive humoral immunity following cICI that is more pronounced in TOX than
296 NOTx, although no changes of B cell abundances were observed in peripheral blood.
297

298 **Regulatory activity by Tregs is preserved upon systemic inflammation in the context of irAEs**

299 Finally, we sought to characterize the response of regulatory T (Treg) cells after ICI treatment.
300 Abundance of forkhead box protein 3 $(FOXP3)^{+}$ $CD25^{+}$ $CD4^{+}$ Tregs increased over time, especially in
301 cICI TOX patients (**Fig. 6a**). Already at baseline, Tregs from patients showed higher expression of T-
302 box transcription factor TBX21 (T-bet) compared with healthy donors (**Fig. 6b**). This may be indicative
303 of a more activated Th1-polarized state, even before the introduction of ICI. To assess whether Tregs
304 can adequately respond to systemic inflammation inflicted by ICI, we compared expression levels of co-
305 inhibitory and co-stimulatory receptors. At Timepoint 3/Toxicity, mainly cICI TOX patients clustered
306 together, marked by upregulation of CTLA-4, ICOS and TIGIT (**Fig. 6c**). Notably, the only two cICI TOX
307 patients with grade 4 irAEs clustered distinctly, characterized by Tregs that failed to upregulate CTLA-
308 4 or TIGIT. In sum, these findings indicate that peripheral Treg function upon systemic inflammation is
309 generally preserved after ICI, while Treg dysfunction may contribute to more severe irAEs.
310

311 **Discussion**

312 Longitudinal studies into mechanisms underlying irAEs can importantly contribute to establishing
313 evidence-based treatment strategies. Therefore, we studied lymphocyte dynamics in peripheral blood
314 of healthy donors and ICI-treated patients with and without irAEs from baseline to several weeks into
315 treatment. Key findings are that cycling Th1-associated effector memory $CD4^{+}$ T cells appear important
316 drivers of acute irAEs, specifically in cICI. Besides, Th17- and Th2-associated responses contribute to
317 the development of irAEs following cICI, but no changes in abundance or activation of B cell subsets
318 were found. In contrast, anti-PD-1-associated irAEs were characterized by a modestly enhanced Th1
319 response compared to anti-PD-1-treated patients without irAEs. This likely relates to the less acute
320 nature of anti-PD-1 associated toxicity. We showed that peripheral blood $PD\text{-}1^{+}LAG\text{-}3^{+}$ $CD8^{+}$ T cells

321 retained their proinflammatory potential and that especially within this DP subset the fraction of
322 granzyme B producing cells increases towards cICI TOX relative to other patient groups.

323 Our key findings are corroborated by a recent study which showed that irAEs are associated
324 with early proliferation of peripheral blood (activated) $CD4^+$ and $CD8^+$ T cell subsets in a Th1-skewed
325 milieu (based on serum CXCL9/10/11 and IFN-γ) [9]. In contrast to our findings, this group also found a
326 cellular Th1-associated response for irAEs after anti-PD-1. This may be due to the difference in sampling
327 of the first on-treatment timepoint at 7-14 days in [9] versus ±3 weeks in our study. Indeed, Nuñez et al.
328 found that at later timepoints the percentage activated $CD4^+$ and $CD8^+$ of all T cells had returned to
329 baseline levels in patients with irAEs [9]. This also fits the observation that cycling $CD8^+$ T cells peak at
330 seven days after anti-PD-1 treatment before they gradually return towards baseline levels three weeks
331 post-treatment [31], possibly because of migration of proliferating cells into tissues.

332 ICI may induce proliferation and reinvigorate antitumor responses in different non-terminally
333 exhausted cell populations, including PD-1^+ $CD8^+$ T cells [32, 33]. We showed that PD-1^+LAG-3^+ (DP) T
334 cells produced highest amounts of IFN-γ after restimulation, which may indicate intact proinflammatory
335 potential *in vivo*. However, phenotypically similar T cells may exert differential function dependent on
336 location [34]. Besides, despite T cell transcriptomic overlap of proinflammatory genes and exhaustion
337 markers [35, 36], *ifng* translation may be hampered in dysfunctional T cells [37]. In addition to IFN-γ
338 production, cICI TOX featured a profound increase in granzyme B production over time, especially in
339 DP $CD8^+$ T cells, which could indicate reinvigoration of dysfunctional cells and *de novo* activation. In
340 sum, our study presents DP T cells as most potent proinflammatory and cytotoxic cells, but to what
341 extent this potential is deployed *in vivo* likely depends on ICI regimen.

342 We observed ongoing proliferation in the $CD8^+$ and, most prominently, $CD4^+$ memory pools in
343 cICI TOX. Our results are consistent with other studies indicating increased $CD4^+$ and $CD8^+$ clonal
344 expansion and repertoire diversification in patients with irAEs [10, 15, 38-40]. Moreover, $CD4_{EM}$ T cell
345 expansion in patients with irAEs parallels CD4 memory abundance in classical autoimmune disease
346 [10]. Together, these data reinforce the hypothesis that cross- or autoreactive $CD4_{EM}$ clones may be
347 unleashed upon ICI treatment in some, especially early, irAEs.

348 Helper T cells may also provide help to autoantibody-producing B cells. In line with an antibody-
349 mediated etiology, our serum cytokine data (including CXCL13 and IL-21) suggest germinal center
350 activation or TLS formation both in cICI and anti-PD-1 monotherapy irAEs. $CD4_{EM}$ T cells have been

351 shown to contribute to thyroiditis development in anti-PD-1 treated mice with preexisting autoimmunity
352 following anti-thyroglobulin immunization [13]. Recent work by Johannet et al. showed that baseline
353 serum autoantibody signatures are predictive of severe irAEs (not limited to thyroiditis) with adjuvant
354 anti-PD-1 and/or anti-CTLA-4 [41], which presents further evidence that preexistent subclinical
355 autoimmunity may be at the root of various irAEs. Importantly, CXCL13 increase does not *per se* indicate
356 TLS formation, as tumor-reactive T cells identified through *CXCL13* expression can also be a source
357 that expands upon treatment in ICI-responders [42].

358 The role of B cells in irAE development is further solidified by human data on increasing $CD21^{lo}$
359 B cells in association with irAEs in the setting of cICI [11, 30]. We were not able to reproduce these
360 findings, which may be due to different timing in blood collection and B cells migrating into peripheral
361 tissues shortly following activation. A recent study found that aged anti-PD-1-treated mice developed
362 TLS-like aggregates in irAE-affected tissue in a CXCL13-dependent fashion and that B cell depletion
363 could attenuate ICI-inflicted toxicity [43]. So far, the use of rituximab for irAE management is limited to
364 case reports [44]. These data together with our work reinforce B cells as a potential target for irAE
365 treatment, although caution is warranted as TLS activation has also been strongly associated with
366 clinical response to ICI [45].

367 Strengths of our study include the longitudinal design with multiple on-treatment timepoints, the
368 stratified analysis for anti-PD-1 and combined ICI treatment and the variety of measured T and B cell
369 parameters. This allowed investigation of very early treatment-specific immunological effects that
370 precede irAE onset. Our study has several limitations. First, age and sex were unevenly distributed
371 among groups. Second, there was considerable heterogeneity in type of irAEs, also within different
372 strata. However, this simultaneously presents as a strength: we clearly found significant and clinically
373 relevant differences between groups that would be less generalizable to the general irAE patient
374 population if obtained within a controlled and irAE-homogenized cohort. Third, our study was powered
375 to discover irAE-related differences stratified by ICI regimen. Therefore, it did not allow for further
376 stratification by ICI response, which would moreover require restriction to a single tumor type. Lastly,
377 our research was limited to the peripheral blood compartment.

378 In conclusion, we show that the peripheral blood immune response substantially differs between
379 patients treated with cICI and anti-PD-1 monotherapy, and between cICI-treated patients with and
380 without irAEs. Toxicity is clearly dominated by enhanced Th1-associated immunity, but we showed that

381 the Th17 pathway and germinal center activation also contribute to cICI toxicity. In this way, our study
382 provides rationale to guide irAE treatment schemes based on ICI regimen and to deploy specific T-cell-
383 directed (second-line) strategies, such as anti-IL-6R, especially in cICI-associated irAEs.
384
385 **Figure legends**
386 **Figure 1 Design of multicolor longitudinal flow cytometry study**. Peripheral blood mononuclear cell
387 (PBMC) and serum samples from immune checkpoint inhibitor (ICI)-treated patients developing or
388 remaining free of clinically relevant immune-related adverse events (irAEs) were included at baseline,
389 ±3 weeks into treatment and at ±6 weeks or upon irAE onset (for which median time-to-onset and inter-
390 quartile range are shown). Healthy donor PBMCs and serum were included for comparison. Created
391 with BioRender.com.
392
393 **Figure 2 Effector memory $CD4^+$ T cell proliferation increases over time in combined-ICI treated**
394 **patients with toxicity, relative to other groups, and is at baseline associated with early irAE**
395 **onset.** (**a**) Plot showing clustering of different groups in principal component analysis (PCA) with pooled
396 flow cytometric data including all 159 readout parameters across panels. (**b**) Individual patient
397 trajectories of the percentage $Ki67^+$ of $CD4^+$ effector memory ($CD4_{EM}$) T cells. Comparison by unpaired
398 Wilcoxon test because of missing paired data for some patients. (**c**,**d**) Percentage proliferating of total
399 $CD4_{EM}$ (**c**) and $CD8_{EM}$ (**d**) T cells over time. Only significant coefficients from mixed-effects models for
400 the interaction term with time ('B'), indicating statistically significant change compared to other groups,
401 are shown. Gray solid and dashed lines indicate mean healthy donor level with 95% confidence interval.
402 (**e**) Correlation between baseline CD_{EM} proliferation rate and time-to-toxicity, stratified by ICI-regimen
403 (by Spearman correlation). irAE: immune-related adverse event, NS: not significant, w/o: without, *
404 $P<0.05$
405
406 **Figure 3 Both Th1- and Th17-associated immune responses are observed in combined-ICI**
407 **treated patients with toxicity, whereas only enhanced Th1-associated immunity is associated**
408 **with anti-PD-1 associated toxicity.** (**a**,**b**) Percentage IFN-γ^+ of total $CD4^+$ T cells (**a**) and percentage
409 proliferating of $CXCR3^+CCR4^-$ Th1-associated $CD4^+$ T cells (**b**) over time. Only significant coefficients
410 from mixed-effects models for the interaction term with time ('B'), indicating statistically significant

411 change compared to other groups, are shown. Gray solid and dashed lines indicate mean healthy donor
412 level with 95% confidence interval. (**c**) Heatmap showing serum levels of cytokines and chemokines
413 after ±6 weeks (T3), upon irAE onset (Toxicity) or in healthy donors. Data are scaled by individual
414 proteins across timepoints (see **Supplementary Fig. 3b**,**c**), enabling direct comparison of individual
415 proteins between three timepoints. Unsupervised clustering of patients by Manhattan distance. (**d**)
416 Volcano plot showing relative increase in serum protein levels at Timepoint 3/Toxicity in all patients with
417 irAEs (TOX; anti-PD-1 and cICI combined) versus all patients without irAEs (NOTx). Full protein names
418 are in **Supplementary Table 2**. (**e**) Fold-change in percentage IL-17$^+$ of CD4$^+$ T cells relative to baseline
419 in cICI-treated patients without irAEs (left; NOTx) and with (right; TOX) irAEs. irAE: immune-related
420 adverse event, NS: not significant, w/o: without.
421
422 **Figure 4 PD-1$^+$LAG-3$^+$ double positive CD8$^+$ memory T cells retain their inflammatory potential**
423 **regardless the development of toxicity.** (**a**) Representative flow cytometry plot of CD95 and CD45RO
424 expression in CD8$^+$ T cells. (**b**) t-SNE visualizations for a random 10% subset of all CD3$^+$ T cells from
425 all patients at Timepoint 3/Toxicity and healthy donors, with relative abundance shown in density plots
426 (top) and expression of lineage markers, IFN-γ and granzyme B in overlay plots (bottom). (**c**) Baseline
427 percentages of CD45RO$^+$ CD4$^+$ (left) and CD95$^+$ CD8$^+$ (right) T cells positive for PD-1 alone or PD-1
428 and LAG-3. Comparisons by Kruskal-Wallis tests. (**d**,**e**) Percentages of CD95$^+$CD8$^+$ T cells producing
429 IFN-γ after PMA/ionomycin stimulation, depending on inhibitory receptor expression pattern, in patients
430 without (**d**) or with irAEs (**e**) stratified by time of sample collection; anti-PD-1- and cICI-treated patients
431 are combined. Comparisons by pairwise paired Wilcoxon tests with Benjamini-Hochberg correction for
432 multiple testing. (**f**) Percentage of granzyme B producing PD-1$^+$LAG-3$^+$ CD95$^+$CD8$^+$ T cells over time.
433 Significant coefficient (interaction term with time; 'B') from mixed-effects model is shown. Gray solid and
434 dashed lines indicate mean healthy donor level with 95% confidence interval. cICI: combined ICI, irAE:
435 immune-related adverse event, NS: not significant, w/o: without. * P<0.05, ** P<0.01, *** P<0.001, ****
436 P<0.0001.
437
438 **Figure 5 Increasing serum CXCL13 levels and higher baseline plasmablast abundance in**
439 **patients with early toxicity suggest a role for adaptive humoral immunity in toxicity after**
440 **combined ICI.** (**a**-**c**) Percentages of CD21^{lo} (**a**) and CD27$^+$ memory (**b**) B cells of total B cells and serum

level (in pg/ml) of CXCL13 (**c**) over time. Only significant coefficients (interaction terms with time; 'B') from mixed-effects models are shown. Gray solid and dashed lines indicate mean healthy donor level with 95% confidence interval. (**d**) Correlation between baseline percentage $CD27^{+}CD38^{hi}$ plasmablasts of total B cells and time-to-toxicity, stratified by ICI-regimen (by Spearman correlation). irAE: immune-related adverse event, w/o: without.

Figure 6 Peripheral regulatory T cell abundance and function are generally preserved upon toxicity. (**a**) Percentage of $CD25^{+}FOXP3^{+}$ $CD4^{+}$ Treg cells of total $CD4^{+}$ T cells over time. Significant coefficient (interaction term with time; 'B') from mixed-effects model is shown. Gray solid and dashed lines indicate mean healthy donor level with 95% confidence interval. (**b**) Comparison of median fluorescence intensity (MFI) of T-bet in Tregs at baseline between healthy donors and all ICI-treated patients, by Wilcoxon test. (**c**) Expression levels (by MFI) of inhibitory and costimulatory receptors in Tregs (for patients Timepoint 3/Toxicity), hierarchically clustered by Euclidean distance. irAE: immune-related adverse event, w/o: without.

References

1. Sullivan RJ, Weber JS. Immune-related toxicities of checkpoint inhibitors: mechanisms and mitigation strategies. Nat Rev Drug Discov 2022;21(7):495-508. doi:10.1038/s41573-021-00259-5
2. Haanen JBAG, Carbonnel F, Robert C, et al. Management of toxicities from immunotherapy: ESMO Clinical Practice Guidelines for diagnosis, treatment and follow-up. Ann Oncol 2018;29:iv264-iv266. doi:10.1093/annonc/mdy162.
3. Schneider BJ, Naidoo J, Santomasso BD, et al. Management of Immune-Related Adverse Events in Patients Treated With Immune Checkpoint Inhibitor Therapy: ASCO Guideline Update. J Clin Oncol 2021;39(36):4073-4126. doi:10.1200/JCO.21.01440
4. Brahmer JR, Abu-Sbeih H, Ascierto PA, et al. Society for Immunotherapy of Cancer (SITC) clinical practice guideline on immune checkpoint inhibitor-related adverse events. J Immunother Cancer 2021;9(6):e002435. doi:10.1136/jitc-2021-002435
5. Verheijden RJ, May AM, Blank CU, et al. Association of Anti-TNF with Decreased Survival in Steroid Refractory Ipilimumab and Anti-PD1-Treated Patients in the Dutch Melanoma Treatment Registry. Clin Cancer Res 2020;26(9):2268-2274. doi:10.1158/1078-0432.CCR-19-3322

471 6. van Not OJ, Verheijden RJ, van den Eertwegh AJM, et al. Association of Immune-Related Adverse
472 Event Management With Survival in Patients With Advanced Melanoma. JAMA Oncol
473 2022;8(12):1794-1801. doi:10.1001/jamaoncol.2022.5041
474 7. Hommes JW, Verheijden RJ, Suijkerbuijk KPM, Hamann D. Biomarkers of Checkpoint Inhibitor
475 Induced Immune-Related Adverse Events—A Comprehensive Review. Front Oncol
476 2021;10:585311. doi:10.3389/fonc.2020.585311
477 8. Nuñez NG, Berner F, Friebel E, et al. Immune signatures predict development of autoimmune toxicity
478 in patients with cancer treated with immune checkpoint inhibitors. *Med (N Y)*. 2023;4(2):113-129.e7.
479 doi:10.1016/j.medj.2022.12.007
480 9. Chaput N, Lepage P, Coutzac C, et al. Baseline gut microbiota predicts clinical response and colitis
481 in metastatic melanoma patients treated with ipilimumab. Ann Oncol 2017;28(6):1368-1379.
482 doi:10.1093/annonc/mdx108
483 10. Lozano AX, Chaudhuri AA, Nene A, et al. T cell characteristics associated with toxicity to immune
484 checkpoint blockade in patients with melanoma. Nat Med 2022;28(2):353-362. doi:10.1038/s41591-
485 021-01623-z
486 11. Das R, Bar N, Ferreira M, et al. Early B cell changes predict autoimmunity following combination
487 immune checkpoint blockade. J Clin Invest 2018;128(2):715-720. doi:10.1172/JCI96798
488 12. Kim KH, Hur JY, Cho J, et al. Immune-related adverse events are clustered into distinct subtypes by
489 T-cell profiling before and early after anti-PD-1 treatment. Oncoimmunology 2020;9(1):e1722023.
490 doi:10.1080/2162402X.2020.1722023
491 13. Yasuda Y, Iwama S, Sugiyama D, et al. CD4 $^{+}$ T cells are essential for the development of destructive
492 thyroiditis induced by anti–PD-1 antibody in thyroglobulin-immunized mice. Sci Transl Med
493 2021;13(593): eabb7495. doi:10.1126/scitranslmed.abb7495
494 14. Hutchinson JA, Kronenberg K, Riquelme P, et al. Virus-specific memory T cell responses unmasked
495 by immune checkpoint blockade cause hepatitis. Nat Commun 2021;12(1):1439.
496 doi:10.1038/s41467-021-21572-y
497 15. Oh DY, Cham J, Zhang L, et al. Immune Toxicities Elicted by CTLA-4 Blockade in Cancer Patients
498 Are Associated with Early Diversification of the T-cell Repertoire. Cancer Res 2017;77(6):1322-1330.
499 doi:10.1158/0008-5472.CAN-16-2324

500 16. Berner F, Bomze D, Diem S, et al. Association of Checkpoint Inhibitor-Induced Toxic Effects with
501 Shared Cancer and Tissue Antigens in Non-Small Cell Lung Cancer. JAMA Oncol 2019;5(7):1043-
502 1047. doi:10.1001/jamaoncol.2019.0402
503 17. Johnson DB, Balko JM, Compton ML, et al. Fulminant Myocarditis with Combination Immune
504 Checkpoint Blockade. N Engl J Med 2016;375(18):1749-1755. doi:10.1056/NEJMoa1609214
505 18. Bayless NL, Bluestone JA, Bucktrout S, et al. Development of preclinical and clinical models for
506 immune-related adverse events following checkpoint immunotherapy: a perspective from SITC and
507 AACR. J Immunother Cancer 2021;9(9):e002627. doi:10.1136/jitc-2021-002627
508 19. Eisenhauer EA, Therasse P, Bogaerts J, et al. New response evaluation criteria in solid tumours:
509 Revised RECIST guideline (version 1.1). Eur J Cancer 2009;45(2):228-247.
510 doi:10.1016/j.ejca.2008.10.026
511 20. NCI (National Cancer Institute). Common Terminology Criteria for Adverse Events (CTCAE) v5.0
512 [online]. 2017. https://ctep.cancer.gov/protocoldevelopment/electronic_applications/ctc.htm#ctc_50.
513 21. Kamphorst AO, Pillai RN, Yang S, et al. Proliferation of PD-1+ CD8 T cells in peripheral blood after
514 PD-1–targeted therapy in lung cancer patients. Proc Natl Acad Sci U S A 2017;114(19):4993-4998.
515 doi:10.1073/pnas.1705327114
516 22. de Jager W, Prakken BJ, Bijlsma JWJ, Kuis W, Rijkers GT. Improved multiplex immunoassay
517 performance in human plasma and synovial fluid following removal of interfering heterophilic
518 antibodies. J Immunol Methods 2005;300(1-2):124-135. doi:10.1016/j.jim.2005.03.009
519 23. Scholman RC, Giovannone B, Hiddingh S, et al. Effect of anticoagulants on 162 circulating immune
520 related proteins in healthy subjects. Cytokine 2018;106:114-124. doi:10.1016/j.cyto.2017.10.021
521 24. van Gassen S, Callebaut B, van Helden MJ, et al. FlowSOM: Using self-organizing maps for
522 visualization and interpretation of cytometry data. Cytometry A 2015;87(7):636-645.
523 doi:10.1002/cyto.a.22625
524 25. Luke SG. Evaluating significance in linear mixed-effects models in R. Behav Res Methods
525 2017;49(4):1494-1502. doi:10.3758/s13428-016-0809-y
526 26. Martins F, Sofiya L, Sykiotis GP, et al. Adverse effects of immune-checkpoint inhibitors:
527 epidemiology, management and surveillance. Nat Rev Clin Oncol 2019;16(9):563-580.
528 doi:10.1038/s41571-019-0218-0

529 27. Hailemichael Y, Johnson DH, Abdel-Wahab N, et al. Interleukin-6 blockade abrogates
530 immunotherapy toxicity and promotes tumor immunity. Cancer Cell 2022;40(5):509-523.e6.
531 doi:10.1016/j.ccell.2022.04.004
532 28. Galletti G, de Simone G, Mazza EMC, et al. Two subsets of stem-like CD8+ memory T cell
533 progenitors with distinct fate commitments in humans. Nat Immunol 2020;21(12):1552-1562.
534 doi:10.1038/s41590-020-0791-5
535 29. Simon S, Voillet V, Vignard V, et al. PD-1 and TIGIT coexpression identifies a circulating CD8 T cell
536 subset predictive of response to anti-PD-1 therapy. J Immunother Cancer 2020;8(2):e001631.
537 doi:10.1136/jitc-2020-001631
538 30. Nishimura K, Konishi T, Ochi T, et al. CD21lo B Cells Could Be a Potential Predictor of Immune-
539 Related Adverse Events in Renal Cell Carcinoma. J Pers Med 2022;12(6):888.
540 doi:10.3390/jpm12060888
541 31. Kim KH, Cho J, Ku BM, et al. The First-week Proliferative Response of Peripheral Blood PD-1+CD8+
542 T Cells Predicts the Response to Anti-PD-1 Therapy in Solid Tumors. Clin Cancer Res
543 2019;25(7):2144-2154. doi:10.1158/1078-0432.CCR-18-1449
544 32. Huang AC, Postow MA, Orlowski RJ, et al. T-cell invigoration to tumour burden ratio associated with
545 anti-PD-1 response. Nature 2017;545(7652):60-65. doi:10.1038/nature22079
546 33. Huang AC, Orlowski RJ, Xu X, et al. A single dose of neoadjuvant PD-1 blockade predicts clinical
547 outcomes in resectable melanoma. Nat Med 2019;25(3):454-461. doi:10.1038/s41591-019-0357-y
548 34. Wu X, Zhang H, Xing Q, et al. PD-1+ CD8+ T cells are exhausted in tumours and functional in
549 draining lymph nodes of colorectal cancer patients. Br J Cancer 2014;111(7):1391-1399.
550 doi:10.1038/bjc.2014.416
551 35. Zheng L, Qin S, Si W, et al. Pan-cancer single-cell landscape of tumor-infiltrating T cells. Science
552 2021;374(6574). doi:10.1126/science.abe6474
553 36. Szabo PA, Levitin HM, Miron M, et al. Single-cell transcriptomics of human T cells reveals tissue and
554 activation signatures in health and disease. Nat Commun 2019;10(1):4706. doi:10.1038/s41467-
555 019-12464-3
556 37. Salerno F, Guislain A, Freen-Van Heeren JJ, Nicolet BP, Young HA, Wolkers MC. Critical role of
557 post-transcriptional regulation for IFN-γ in tumor-infiltrating T cells. Oncoimmunology
558 2019;8(2):e1532762. doi:10.1080/2162402X.2018.1532762

559 38. Arakawa A, Vollmer S, Tietze J, et al. Clonality of CD4+ Blood T Cells Predicts Longer Survival With
560 CTLA4 or PD-1 Checkpoint Inhibition in Advanced Melanoma. Front Immunol 2019;10:1336.
561 doi:10.3389/fimmu.2019.01336
562 39. Robert L, Tsoi J, Wang X, et al. CTLA4 Blockade Broadens the Peripheral T-Cell Receptor
563 Repertoire. Clin Cancer Res 2014;20(9):2424-2432. doi:10.1158/1078-0432.CCR-13-2648
564 40. Subudhi SK, Aparicio A, Gao J, et al. Clonal expansion of CD8 T cells in the systemic circulation
565 precedes development of ipilimumab-induced toxicities. Proc Natl Acad Sci U S A
566 2016;113(42):11919-11924. doi:10.1073/pnas.1611421113
567 41. Johannet P, Liu W, Fenyo D, et al. Baseline Serum Autoantibody Signatures Predict Recurrence and
568 Toxicity in Melanoma Patients Receiving Adjuvant Immune Checkpoint Blockade. Clin Cancer Res
569 2022;28(18):4121-4130. doi:10.1158/1078-0432.CCR-22-0404
570 42. Liu B, Zhang Y, Wang D, Hu X, Zhang Z. Single-cell meta-analyses reveal responses of tumor-
571 reactive CXCL13+ T cells to immune-checkpoint blockade. Nat Cancer 2022;3(9):1123-1136.
572 doi:10.1038/s43018-022-00433-7
573 43. Tsukamoto H, Komohara Y, Tomita Y, et al. Aging-associated and CD4 T-cell–dependent ectopic
574 CXCL13 activation predisposes to anti–PD-1 therapy-induced adverse events. Proc Natl Acad Sci U
575 S A. 2022;119(29). doi:10.1073/pnas.2205378119
576 44. Deftereos SN, Georgonikou D. Effectiveness of rituximab in treating immune-checkpoint-inhibitor-
577 induced immune-related adverse events: results of a systematic review. Ann Oncol 2021;32(2):282-
578 283. doi:10.1016/j.annonc.2020.12.001
579 45. Fridman WH, Meylan M, Petitprez F, Sun CM, Italiano A, Sautès-Fridman C. B cells and tertiary
580 lymphoid structures as determinants of tumour immune contexture and clinical outcome. Nat Rev
581 Clin Oncol 2022;19(7):441-457. doi:10.1038/s41571-022-00619-z
582

583 **Statements & Declarations**

584 **Funding**: This investigator-initiated study received funding from Bristol Myers Squibb (grant number
585 CA209-6JY), paid to institution.

586 **Competing interests**: KPMS has advisory relationships with Bristol Myers Squibb, Novartis, MSD,
587 Pierre Fabre, AbbVie, received honoraria from Novartis, MSD and Roche and received research funding

588 from BMS, Philips and TigaTx. FW has advisory relationships with Janssen and Takeda, and received
589 research funding from Takeda, Galapagos, BMS, Sanofi, and Leo Pharma.
590 **Author contributions**: Conceptualization: FW, KPMS, MJME. Project administration and Resources:
591 RJV, MJME, ASRL, KPMS. Data curation: MJME, SAW, RJV. Formal Analysis: MJME, FW, KPMS.
592 Writing - original draft: MJME. Writing – review and editing: all authors. Supervision: FW, KPMS.
593 **Data availability**: Data and scripts for statistical analysis are available upon reasonable request.
594 **Ethics approval**: This study was approved by the University Medical Center Utrecht biobank committee
595 (TCbio 18-123).
596 **Consent to participate**: All participants provided written informed consent in line with the Declaration
597 of Helsinki.
598 **Acknowledgements**: We thank the patients, their families and caregivers, healthy donors, clinical staff
599 and UNICIT consortium members. We would like to thank the Multiplex Core Facility of the University
600 Medical Center Utrecht for performing the multiplex immunoassays.
601 **Collaborators UNICIT consortium**: Linde Meyaard, Jürgen H.E. Kuball, Bas Oldenburg, Jeanette H.W.
602 Leusen.

Figure 1

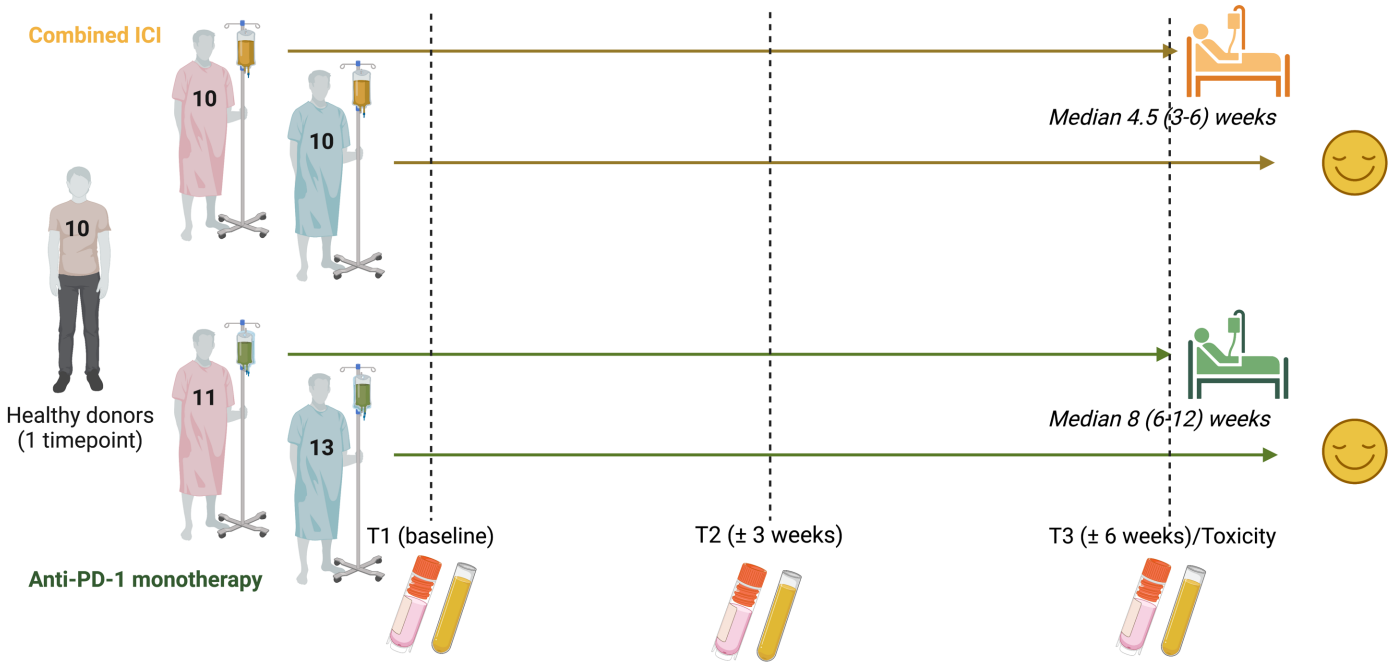
Combined ICI
10
10
10
Median 4.5 (3-6) weeks
Healthy donors
(1 timepoint)
11
13
Median 8 (6-12) weeks
T1 (baseline)
T2 (± 3 weeks)
T3 (± 6 weeks)/Toxicity
Anti-PD-1 monotherapy

Figure 2

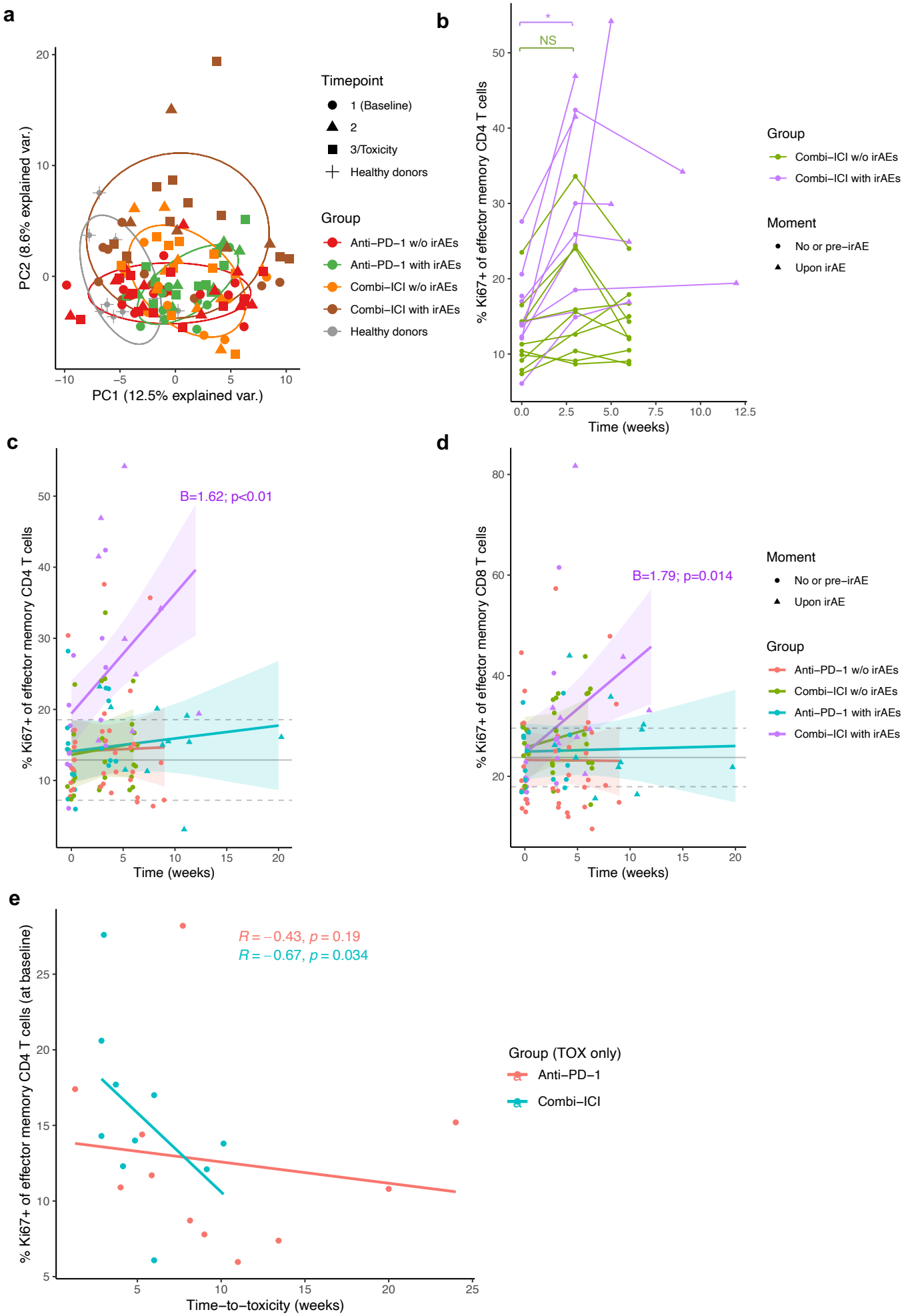
a
PC2 (8.6% explained var.)
PC1 (12.5% explained var.)
Timepoint
1 (Baseline)
2
3/Toxicity
Healthy donors
Group
Anti−PD−1 w/o irAEs
Anti−PD−1 with irAEs
Combi−ICI w/o irAEs
Combi−ICI with irAEs
Healthy donors
b
NS
% Ki67+ of effector memory CD4 T cells
Time (weeks)
Group
Combi−ICI w/o irAEs
Combi−ICI with irAEs
Moment
No or pre−irAE
Upon irAE
c
B=1.62; p<0.01
% Ki67+ of effector memory CD4 T cells
Time (weeks)
d
B=1.79; p=0.014
% Ki67+ of effector memory CD8 T cells
Time (weeks)
Moment
No or pre−irAE
Upon irAE
Group
Anti−PD−1 w/o irAEs
Combi−ICI w/o irAEs
Anti−PD−1 with irAEs
Combi−ICI with irAEs
e
R = −0.43, p = 0.19
R = −0.67, p = 0.034
% Ki67+ of effector memory CD4 T cells (at baseline)
Time−to−toxicity (weeks)
Group (TOX only)
Anti−PD−1
Combi−ICI

Figure 3

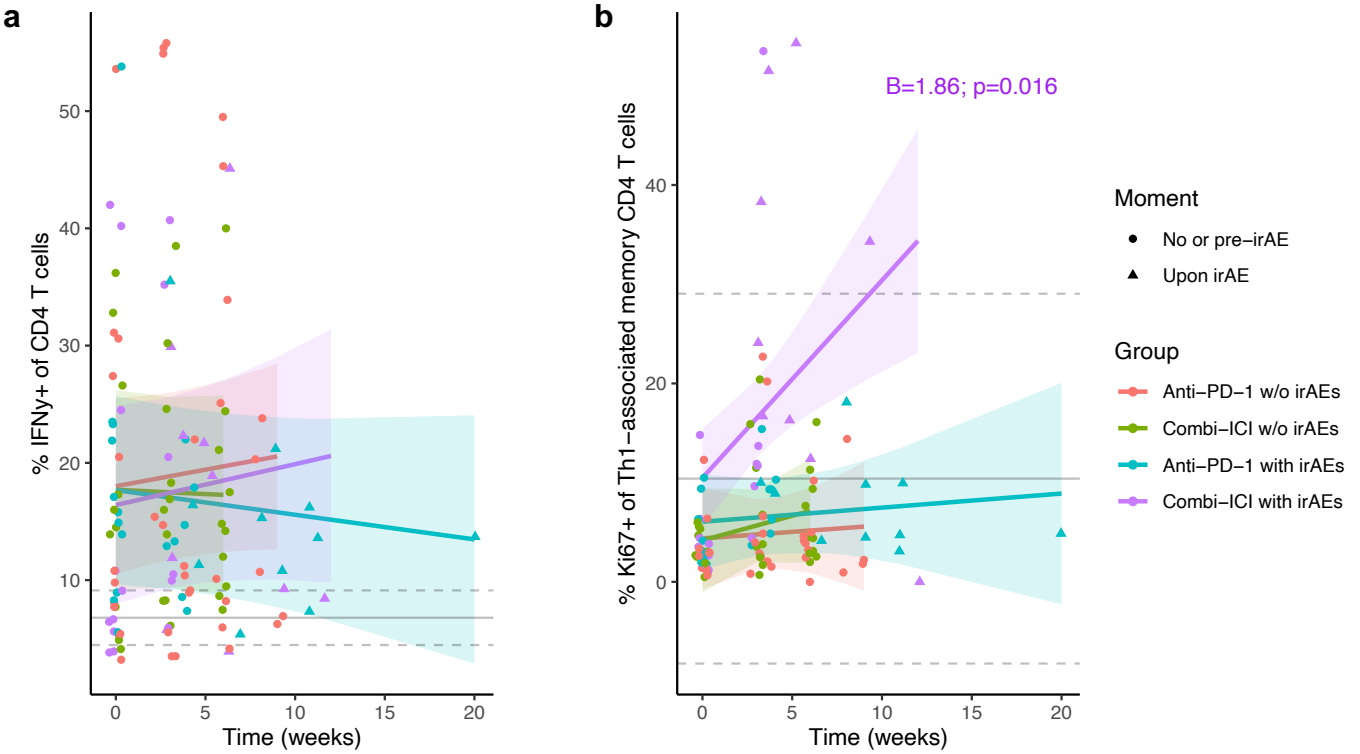
a
% IFNy+ of CD4 T cells
Time (weeks)
b
B=1.86; p=0.016
% Ki67+ of Th1−associated memory CD4 T cells
Time (weeks)
Moment
No or pre−irAE
Upon irAE
Group
Anti−PD−1 w/o irAEs
Combi−ICI w/o irAEs
Anti−PD−1 with irAEs
Combi−ICI with irAEs

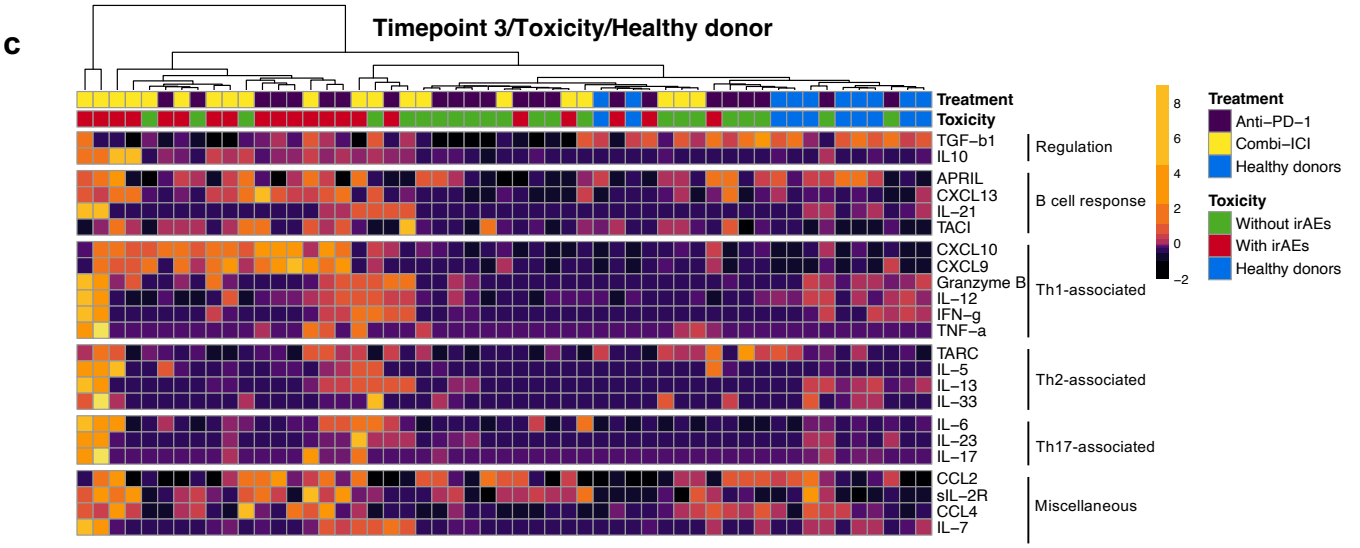
c
Timepoint 3/Toxicity/Healthy donor
Treatment
Toxicity
TGF−b1
IL10
Regulation
APRIL
CXCL13
IL−21
TACI
B cell response
CXCL10
CXCL9
Granzyme B
IL−12
IFN−g
TNF−a
Th1−associated
TARC
IL−5
IL−13
IL−33
Th2−associated
IL−6
IL−23
IL−17
Th17−associated
CCL2
sIL−2R
CCL4
IL−7
Miscellaneous
Treatment
Anti−PD−1
Combi−ICI
Healthy donors
Toxicity
Without irAEs
With irAEs
Healthy donors

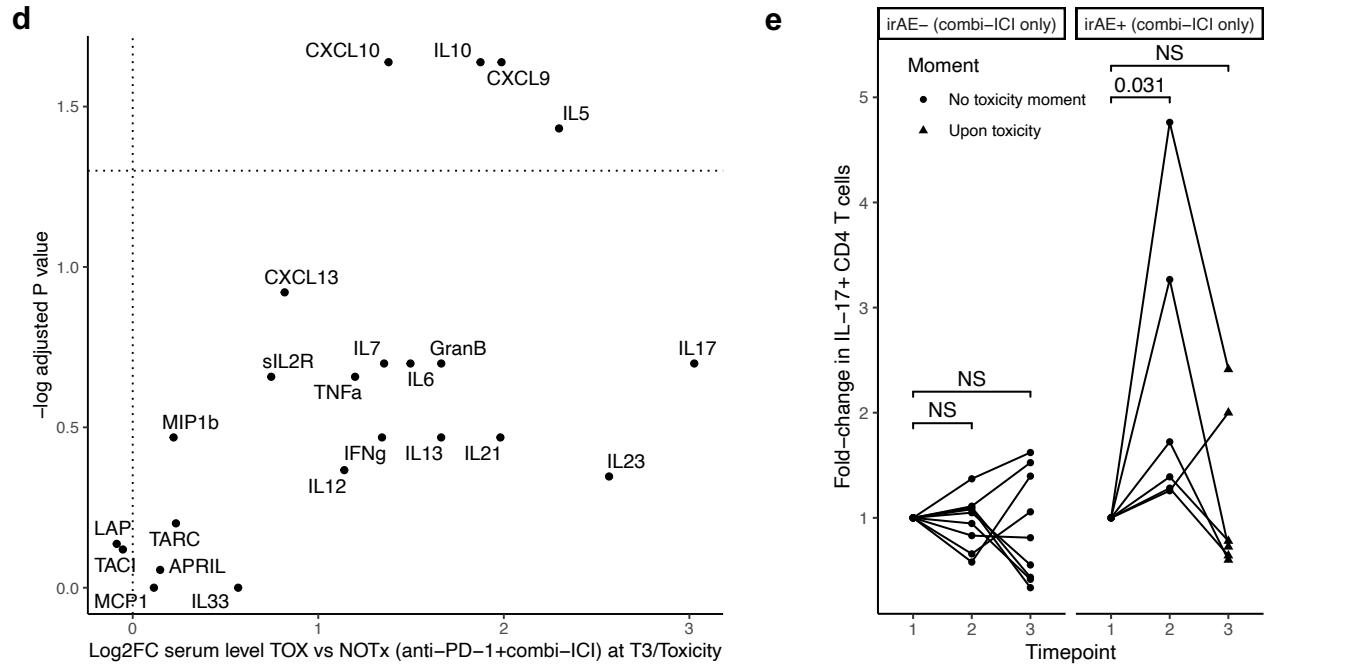
d
−log adjusted P value
Log2FC serum level TOX vs NOTx (anti−PD−1+combi−ICI) at T3/Toxicity
CXCL10
IL10
CXCL9
IL5
CXCL13
IL7
GranB
IL17
sIL2R
IL6
TNFa
MIP1b
IFNg
IL13
IL21
IL23
IL12
LAP
TARC
TACI
APRIL
MCP1
IL33
e
irAE− (combi−ICI only)
irAE+ (combi−ICI only)
Moment
No toxicity moment
Upon toxicity
NS
NS
NS
0.031
Fold−change in IL−17+ CD4 T cells
Timepoint

Figure 4

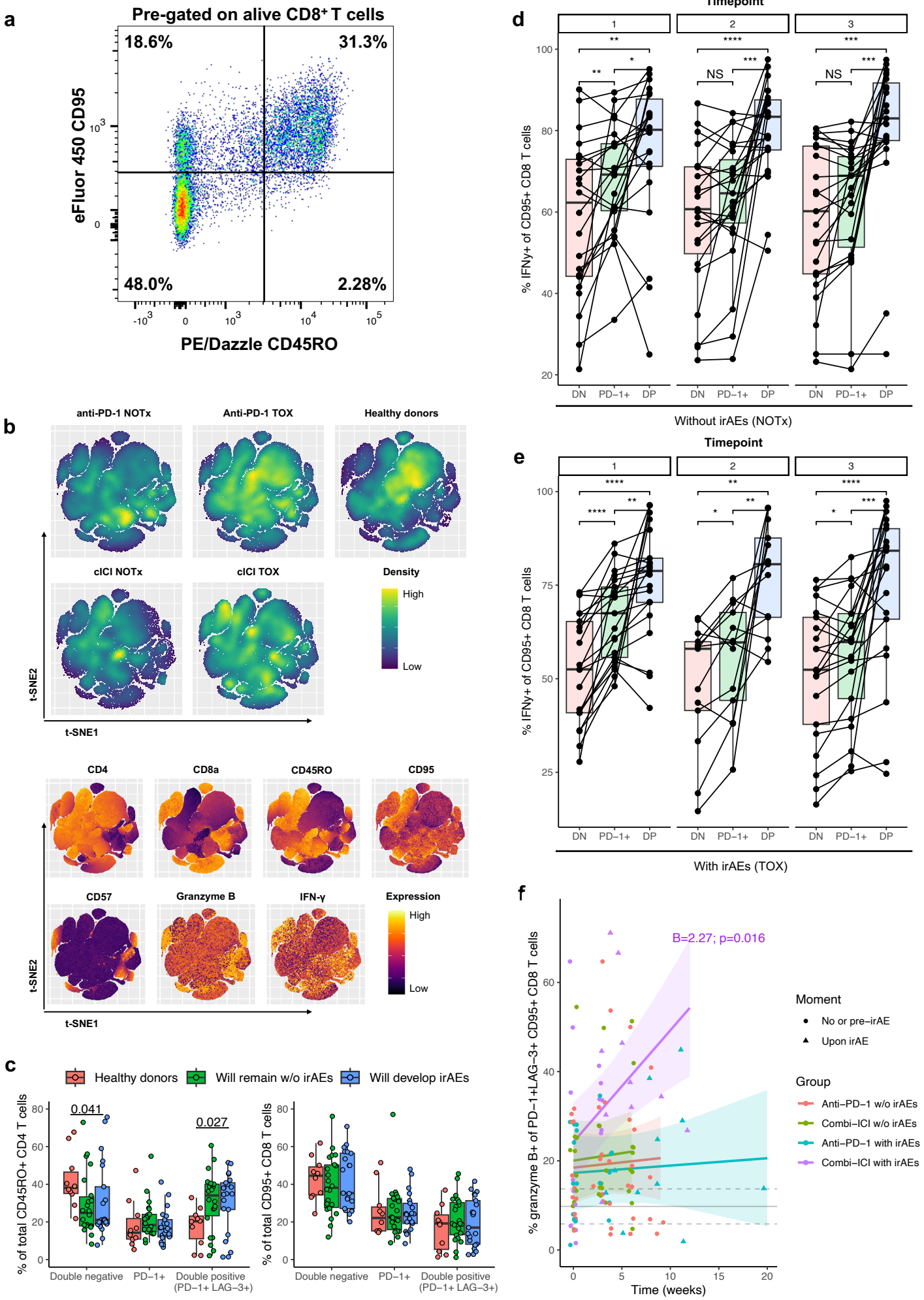
a
Pre-gated on alive CD8+ T cells
18.6%
31.3%
48.0%
2.28%
eFluor 450 CD95
PE/Dazzle CD45RO
b
anti-PD-1 NOTx
Anti-PD-1 TOX
Healthy donors
cICI NOTx
cICI TOX
Density
High
Low
t-SNE2
t-SNE1
CD4
CD8a
CD45RO
CD95
CD57
Granzyme B
IFN-γ
Expression
High
Low
t-SNE2
t-SNE1
c
Healthy donors
Will remain w/o irAEs
Will develop irAEs
0.041
0.027
% of total CD45RO+ CD4 T cells
% of total CD95+ CD8 T cells
Double negative
PD−1+
Double positive (PD−1+ LAG−3+)
d
Timepoint
% IFNγ+ of CD95+ CD8 T cells
DN
PD−1+
DP
NS
Without irAEs (NOTx)
e
Timepoint
% IFNγ+ of CD95+ CD8 T cells
With irAEs (TOX)
f
B=2.27; p=0.016
% granzyme B+ of PD−1+LAG−3+ CD95+ CD8 T cells
Time (weeks)
Moment
No or pre−irAE
Upon irAE
Group
Anti−PD−1 w/o irAEs
Combi−ICI w/o irAEs
Anti−PD−1 with irAEs
Combi−ICI with irAEs

Figure 5

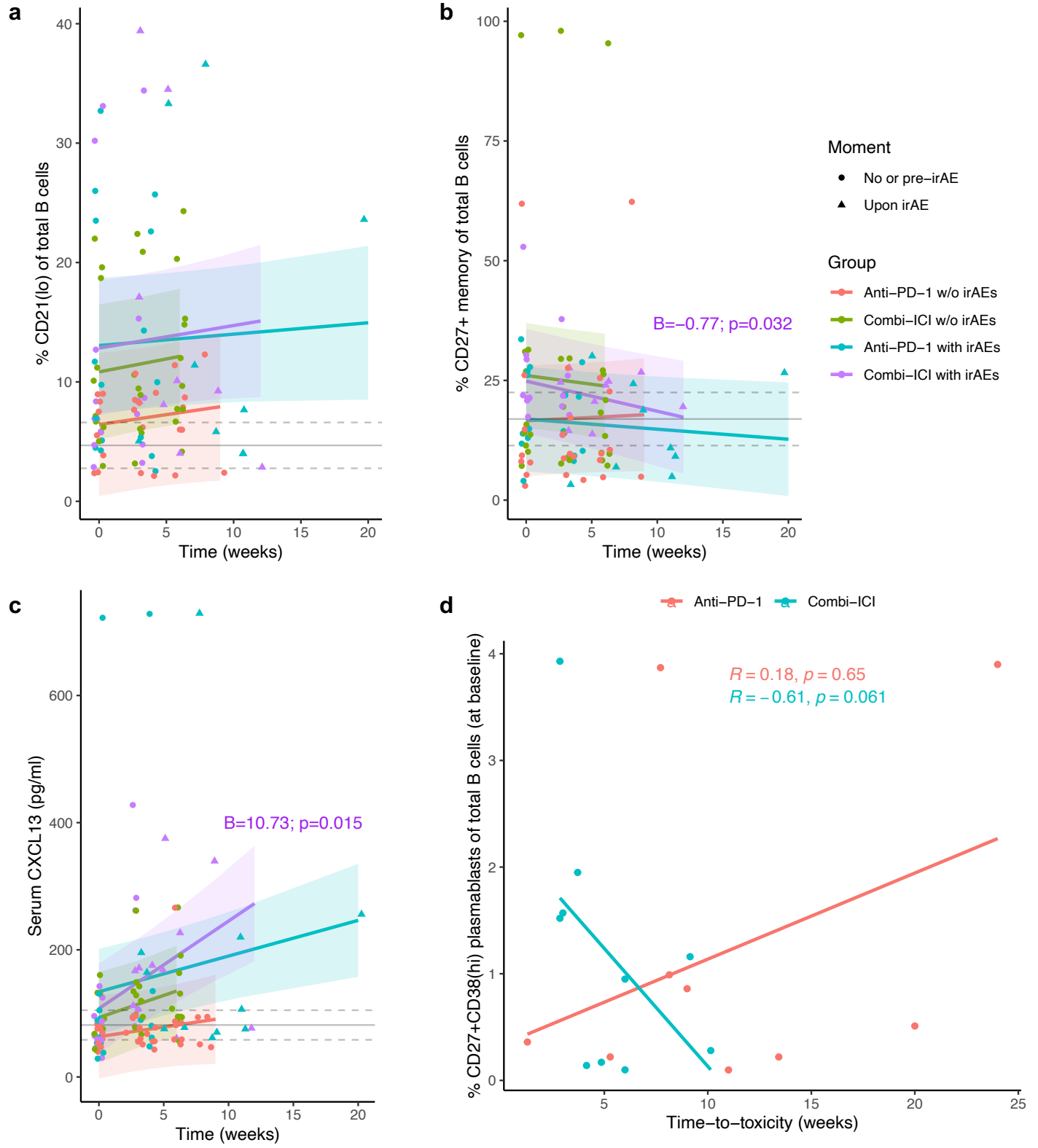
a
% CD21(lo) of total B cells
Time (weeks)
b
% CD27+ memory of total B cells
B=−0.77; p=0.032
Time (weeks)
Moment
No or pre−irAE
Upon irAE
Group
Anti−PD−1 w/o irAEs
Combi−ICI w/o irAEs
Anti−PD−1 with irAEs
Combi−ICI with irAEs
c
Serum CXCL13 (pg/ml)
B=10.73; p=0.015
Time (weeks)
d
Anti−PD−1
Combi−ICI
% CD27+CD38(hi) plasmablasts of total B cells (at baseline)
R = 0.18, p = 0.65
R = −0.61, p = 0.061
Time−to−toxicity (weeks)

Figure 6

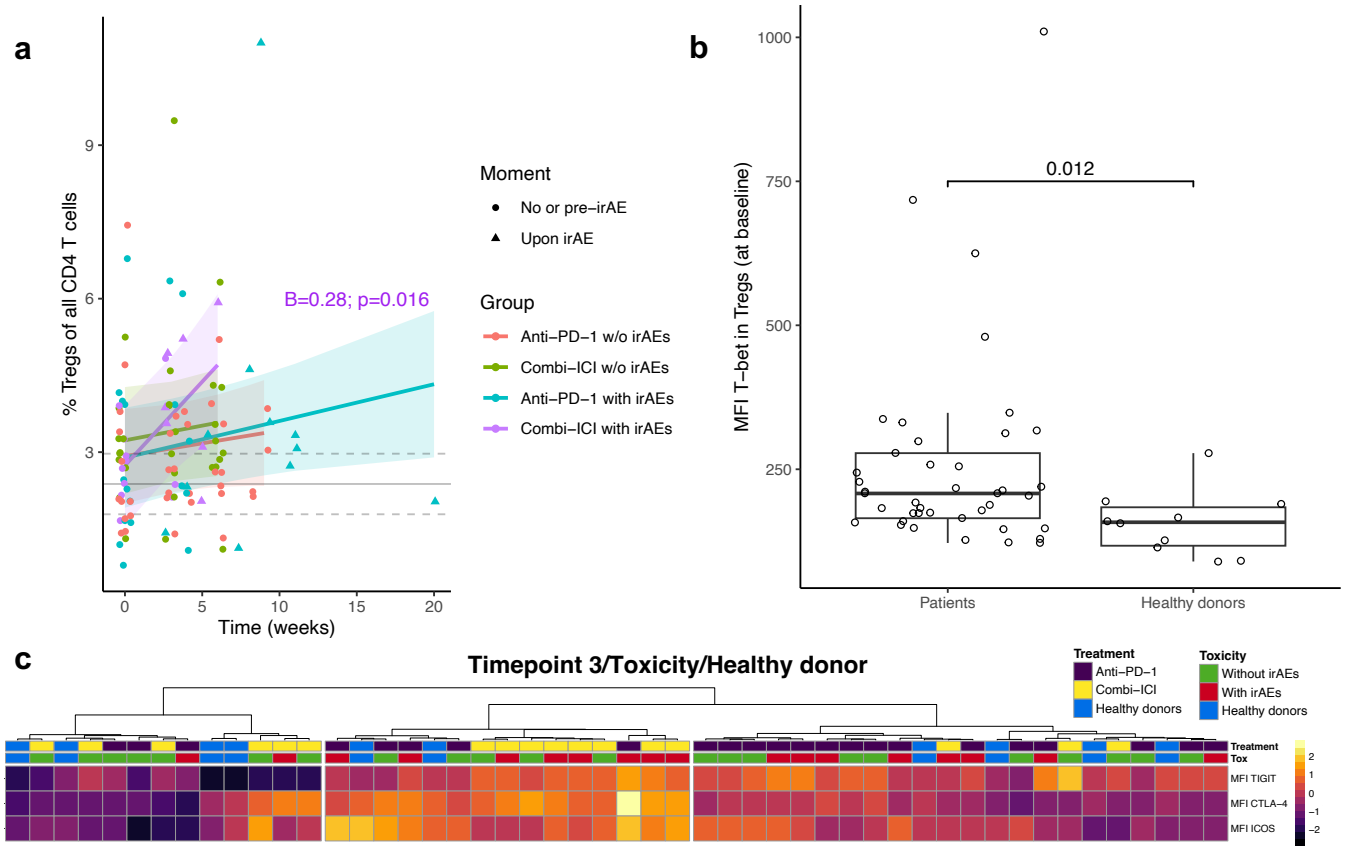
a
% Tregs of all CD4 T cells
Time (weeks)
B=0.28; p=0.016
Moment
No or pre−irAE
Upon irAE
Group
Anti−PD−1 w/o irAEs
Combi−ICI w/o irAEs
Anti−PD−1 with irAEs
Combi−ICI with irAEs
b
MFI T−bet in Tregs (at baseline)
0.012
Patients
Healthy donors
c
Timepoint 3/Toxicity/Healthy donor
Treatment
Anti−PD−1
Combi−ICI
Healthy donors
Toxicity
Without irAEs
With irAEs
Healthy donors
Treatment
Tox
MFI TIGIT
MFI CTLA−4
MFI ICOS